Int J Adv Manuf Technol (2017) 88:1763–1773
DOI 10.1007/s00170-016-8896-6

ORIGINAL ARTICLE

Depth of cut for single abrasive and cutting force in resin bonded diamond wire sawing

Tengyun Liu[1] · **Peiqi Ge**[1,2] · **Yufei Gao**[1,2] · **Wenbo Bi**[1,2]

Received: 21 January 2016 / Accepted: 9 May 2016 / Published online: 23 May 2016

Abstract A new model of calculating depth of cut and cutting force was developed based on indentation fracture mechanics in order to understand the influences of processing parameters on cutting behavior of abrasives in resin bonded diamond wire sawing single crystal silicon. The random distribution characteristic of abrasives and the elasticity of resin layer were taken into account in this model, the correctness of which was verified by using the results from reference under the same processing parameters. Different processing parameter combinations were used to analyze the influences of processing parameters on the depth of cut and cutting force. The obtained results indicated that feed rate and wire speed had different effects on depth of cut and cutting force. The average depth of cut obtained under the condition of considering elasticity of resin layer was less than that got without considering this elasticity. The brittle cutting regime was the major way of material removal for resin bonded diamond wire sawing. The force ratio, total normal force to tangential force, was about 1.2. Finally, a mathematical relationship between cutting force and processing parameters was obtained.

Keywords Resin bonded diamond wire saw · Depth of cut · Cutting force

✉ Peiqi Ge
pqge@sdu.edu.cn

[1] School of Mechanical Engineering, Shandong University, Jinan 250061, China

[2] Key Laboratory of High Efficiency and Clean Mechanical Manufacture, Ministry of Education, Shandong University, Jinan 250061, China

Nomenclature

a	Length of lateral crack
d_{max}	The maximum diameter of abrasive
d_{min}	The minimum diameter of abrasive
d_m	The mean diameter of abrasive
d_{ij}	Diameter of ith abrasive on jth wire cross section
D	Outer diameter of wire
E_1	Elastic modulus of single crystal silicon
E_2	Elastic modulus of resin
F_{n1ij}	Normal force on abrasive by wire
F_{t1ij}	Tangential force on abrasive by wire
F_{n2ij}	Normal force on abrasive by workpiece
F_{t2ij}	Tangential force on abrasive by workpiece
F_N	Total normal force
F_T	Total tangential force
H_{ij}	Protrusion height of abrasive
h_{ij}	Depth of cut for abrasive (indentation depth)
Δh_{ij}	Displacement of abrasive pressed into resin layer
H_1	Hardness of single crystal silicon
h_l	Depth of lateral crack
K_{IC}	Fracture toughness of single crystal silicon
l	The length of wire contacting with workpiece
m	Number of nodes along the radius direction
M	Matrix of abrasive position
n	Number of nodes along the axis direction
N	The total number of diamond grits on the below half of the wire
s	Displacement of wire cross section moving downward
S_{ij}	Cross section area of material which is removed by abrasive
S_{sum}	Total removed cross section area
V_1	Volume of material removed by all abrasive particles
V_2	Volume of wire moving downward
v_f	Feed rate
v_s	Wire speed

α_{ij} Position angle of abrasive
η The density of abrasive particle on wire
θ_{ij} Half tip angle of abrasive
σ Standard deviation for abrasive density function
σ_y Yield stress of single crystal silicon
μ Poisson's ratio of single crystal silicon

1 Introduction

Wire saw, which has several advantages, such as higher efficiency, lower wastage, and being unconstrained by the size of silicon ingot compared to inner diameter saw, has been the main technology of slicing silicon crystal in integrated circuit and PV industries [1]. So far, free abrasive wire saw is the mainstream cutting technology in silicon processing. Besides that, there are two kinds of fixed diamond wire saw: electroplated diamond wire saw and resin bonded diamond wire saw. Slicing wafer with diamond wire saw can reduce the slicing cost and provide a cleaner way of producing wafers [2]. For these two technologies, resin bonded diamond wire saw has some disadvantages; for example, abrasives are less strongly bonded and have shorter service life due to easy wear of the resin layer. However, the resin layer can serve as a cushion and absorb vibration and shock during wire sawing which can result in the reduction of surface damage layer thickness and obtaining a better surface quality. This has been demonstrated by Tsai et al. [3]. A higher surface quality is required to assure the mechanical stability of wafers with the thinness of silicon wafers. According to the study of Watanabe et al. [4], the resin bonded diamond wire saw is suitable for the fabrication of thin solar silicon wafers where the wafer thickness approaches or becomes less than 150 μm.

Many researches have been done on wire saw. The cutting mechanism [5–7], optimization of cutting process [8–11], and the cutting model [12–15] have been studied by experiments and theory. However, most of them are focused on slurry or electroplated diamond wire saw. The resin bonded diamond wire saw has different machining characteristics because of the elasticity of the resin layer. The resin layer can absorb the vibration and shock during slicing, and the abrasives can be pressed into the resin layer when they are forced, which results in reduction of their protrusion heights and decrease in the depth of cut. Fig. 1 shows the surface topography of resin bonded diamond wire saw. It can be seen that the abrasives randomly distribute on the wire and their protrusion heights are small.

There are no ideas on whether the resin bonded diamond wire saw can remove material in ductile regime cutting. The depth of cut for abrasives is a key factor which directly determines the material removal mode. However, it is unable to measure the depth of cut during wire sawing in practice. Gao et al. [16] studied the average depth of cut for abrasives

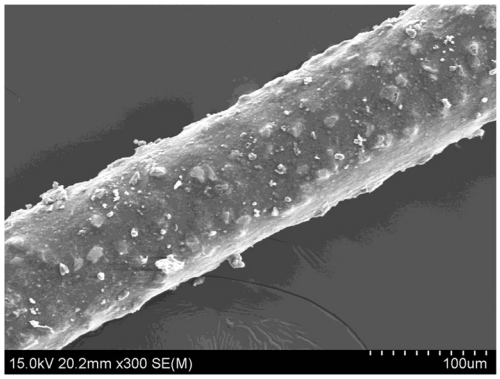

Fig. 1 Resin bonded diamond wire saw

on a cross section of electroplated wire saw. They pointed out that smaller average depth of cut and a higher surface finish would be obtained by using a higher wire speed, lower feed rate, smaller particle size, and more evenly distributed abrasives. Chung et al. [17, 18] established a model of electroplated diamond wire and investigated the depth of cut for a single abrasive particle using a numerical method. The simulation results show that the number of abrasives taking part in removing material is small, and the brittle mode cutting is the main way of removing material.

Cutting force is the main parameter which is the characterization of cutting status and is the major reason to consume energy and generate heat. Researches have been done from the macroscopic [13] or microscopic aspect [19]. For the previous method, experimental measurements are often used. Clark et al. [20, 21] first studied the cutting force of fixed diamond wire saw. Experimental results show that the force ratio of normal force to tangential force is different for different materials. After that, other researchers measured the force when slicing SiC [22, 23]. Their results indicate that the force ratio (normal force to tangential force) is between 0.3 and 1.3 and the main factors affecting cutting force are feed rate and wire speed. On the other hand, from the microscopic view, indentation fracture mechanics is used to analyze the force condition on a single abrasive particle, and the abrasive is usually considered as rigid body [19]. Material removal mode for fixed diamond wire saw is similar to indentation and scratching [24]. Therefore, the conclusions obtained from scratch experiments are used to analyze the force condition of the abrasive during wire sawing.

Up to now, the machining characteristic of abrasives in resin bonded diamond wire sawing was unclear and the relationship between cutting force and machining parameters was limited. Therefore, a study towards this aim was presented in this paper. A new model of calculating depth of cut for abrasive and cutting force based on microscopic view was proposed. The influences of processing parameters on the depth of cut and cutting force were studied, and a mathematical relationship between cutting force and machining parameters was also obtained.

2 Numerical model

2.1 Abrasive shape and size distribution

The shape of diamond abrasives is an important characteristic which can affect the force condition and wear resistance of the abrasive particle. The diamond abrasives have complex and irregular shapes. Generally, the shape of an abrasive particle is sphere or ellipsoid when its diameter is less than 10 nm; the shape of a particle is irregular when its diameter ranges from10 to 100 nm; and an abrasive particle has a regular shape if its diameter is larger than 100 nm [25]. In this paper, we assume that the shape of all abrasive particles is the combination of two cones, as shown in Fig. 2. The diameter of the abrasive is d and the half tip angle is θ.

Based on the study of Sung [26], a higher cutting efficiency and longer service life can be obtained when the protrusion height of the abrasive is between one third and one half of the abrasive size. Moreover, in combination with the study of Watanabe [4], we take the one third to one half of the abrasive size as the protrusion height. The half tip angle θ is taken as a value randomly between 15° and 75° in order to describe the random characteristic.

The diameter of the abrasive particle is the general description of particle size, which is usually denoted by an equivalent diameter. Based on the regulations for diamond abrasives, the sieving method is used to measure the particle size. It is found that the size distribution of abrasive particles is in accordance with normal distribution [27]. Therefore, we adopt the normal distribution to describe the abrasive size. For a given abrasive size, the maximum diameter is d_{max}, the minimum diameter is d_{min}, and the mean diameter is d_m, so,

$$d_m = (d_{\max} + d_{\min})/2 \tag{1}$$

The density function of the abrasive size d is given by

$$f(d) = \frac{1}{\sqrt{2\pi}\sigma} \exp\left\{ -\frac{[d_0 + \log(d)]^2}{2\sigma^2} \right\} \tag{2}$$

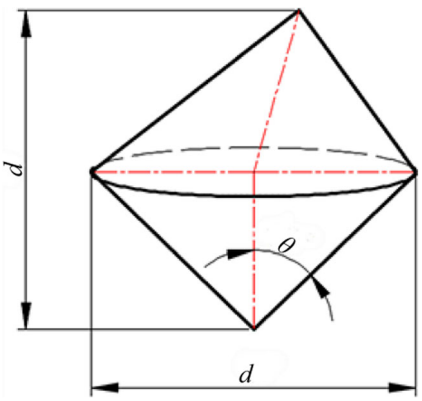

Fig. 2 Model of abrasive particle

Based on the study of Chung [17], the wire saw parameter obtained from SEM is shown in Table 1. It can be seen that the mean diameter of the abrasive is 50 μm. The abrasive diameter follows the normal distribution under a particle size number of abrasive grains. A plot of normal distribution which shows the probability of grain number with different diameters is shown in Fig. 3.

For more precise calculation, the standard deviation σ can be obtained through Fig. 3:

$$\sigma = \frac{d_{\max} - d_{\min}}{6} \tag{3}$$

From this equation, we can obtain that the standard deviation σ is 3.33. So, we take 50 μm as the mean diameter d_m, and the standard deviation σ is 3.33. The abrasive size between 40 and 60 μm will cover 99.73 % of particle sizes, which is in the range of 6σ.

The abrasives embedded into the resin layer are one half to two thirds of the abrasive size; we assume that the thickness of the resin layer is larger than that value, and the distribution of abrasives on wire is shown in Fig. 4.

2.2 Model of resin bonded diamond wire

As shown in Fig. 5, the length of wire contacting with the workpiece is l, and the diameter of wire is D. The wire axially moves with the velocity v_s; at the same time, the workpiece moves along the direction perpendicular to the wire moving direction at the velocity v_f.The density of the abrasive on the wire is η. We assume that the diamond grits on the below half of the wire take part in removing material, so the half part of the wire is only considered. The total number of diamond grits on the below half of the wire is

$$N = \frac{\pi l \eta D}{2} \tag{4}$$

The positions of diamond particles on the wire are random, and their protrusion heights are different too for resin bonded diamond wire. The method, generating a fixed diamond wire saw established by Chung et al. [17], is used in this paper to describe the random positions of the abrasive. By using this method, the wire is full of randomly distributed abrasives with sizes following the normal distribution.

Table 1 Wire saw parameter [17]

Parameters	Value
Wire diameter (μm)	250
Core diameter (μm)	180
Particle size (μm)	40~60
Density (grits/mm^2)	50~70

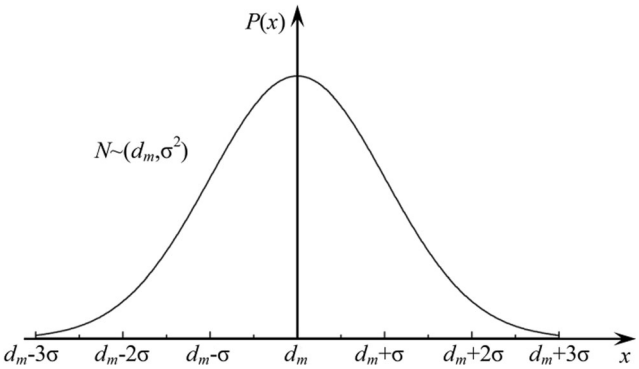

Fig. 3 The abrasive diameter follows Gaussian distribution with the standard deviation σ

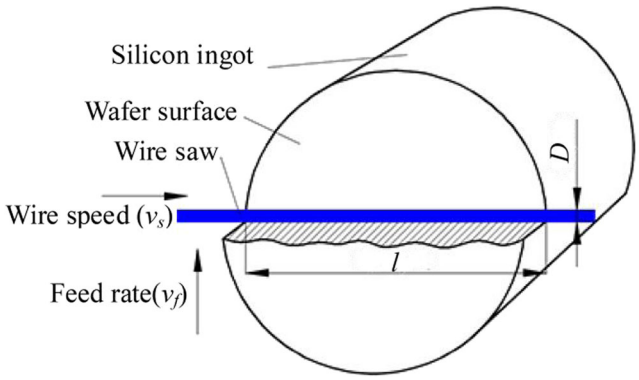

Fig. 5 Model of resin bonded diamond wire sawing silicon ingot

The wire is divided into m × n nodes, where m and n are the number of grids along the radius direction and axis direction, respectively, as shown in Fig. 6. The unit length in both directions must be the same to ensure the equal possibility of the existence of diamond grits in the two directions [17]:

$$\frac{\pi D}{m} = \frac{l}{n} \tag{5}$$

Some modifications are made based on Chung's method. The meshed wire can be seen as a two-dimensional zero matrix, which has m rows and n columns. The method, randomly inserting N numbers in the zero matrix without repetition instead of following the way of judging the probability of the existing grit on a node, is used to describe the random distribution of abrasives. After that, a nonzero matrix is obtained to describe the random position of diamond grits, recorded as matrix M. The nonzero elements, which denote that there is an abrasive in the matrix M, are found by using the loop program, and their corresponding position coordinates are recorded. Then, we define the properties of the abrasive, such as half tip angle, diameter, position angle, and protrusion height. For example, if the position of the nonzero element in M is the ith row and the jth column, the half tip angle of the abrasive is

$$\theta_{ij} = {}^{ij}rand(1) \times \frac{4\pi}{12} + \frac{\pi}{12} \quad (i = 1, 2 \ldots m, j = 1, 2 \ldots n) \tag{6}$$

The diameter of the abrasive particle is

$$d_{ij} = normrnd(d_m, 3.33, [1, 1]) \tag{7}$$

The protrusion height of the abrasive is set as

$$H_{ij} = \left[rand(1) \times \frac{1}{6} + \frac{1}{3} \right] \quad d_{ij} (i = 1, 2 \ldots m, j = 1, 2 \ldots n) \tag{8}$$

The position angle of the abrasive particle on a corresponding cross section is

$$\alpha_{ij} = \frac{\pi(i-1)}{m-1} \quad (i = 1, 2 \ldots m, j = 1, 2 \ldots n) \tag{9}$$

The generated model of resin bonded diamond wire saw is shown in Fig. 7.

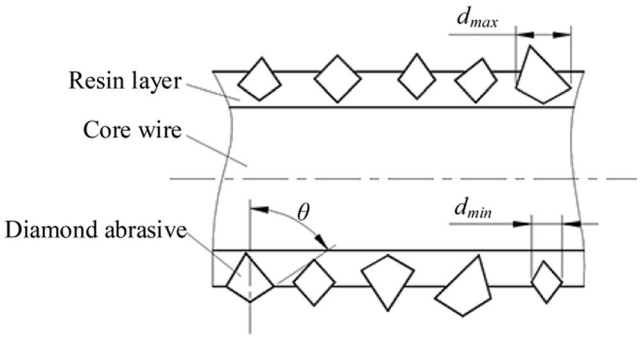

Fig. 4 Abrasive distribution on resin diamond wire saw

2.3 Forces on a single abrasive particle

During the cutting process, the motions of the wire and the workpiece generate normal force and tangential force, taking an abrasive arbitrarily which takes part in cutting material, numbering as M_{ij} (ith abrasive on the jth wire cross section). Because of the movement of the wire, the normal force F_{n1ij} and the tangential force F_{t1ij} are generated. The forces between abrasive and workpiece are complicated. Here, the resultant forces are only considered—normal force F_{n2ij} and tangential force F_{t2ij}—as shown in Fig. 8.

Diamond abrasives can be pressed into the resin layer when it is forced because of the elasticity of resin. As shown in Fig. 8, the displacement of the abrasive pressed into the resin layer is Δh_{ij}, and the depth of cut for the abrasive (indentation depth) is h_{ij}. In theory, the normal force on resin bonded

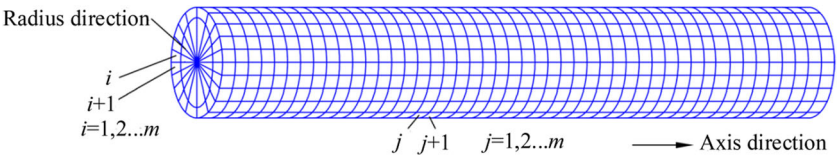

Fig. 6 Grids on resin bonded diamond wire

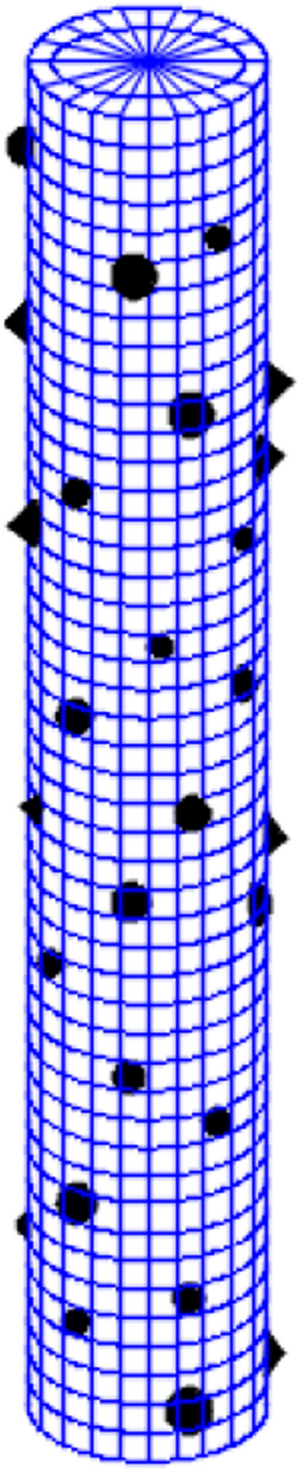

Fig. 7 The model of resin bonded diamond wire saw

diamond wire is equal to the normal force on all abrasives which take part in cutting material.

To simplify the computational model, four forces (F_{n1ij}, F_{t1ij}, F_{n2ij}, and F_{t2ij}) are considered on a single abrasive particle. Based on the equilibrium of forces, we can obtain the following formula:

$$F_{n1ij} = F_{n2ij} \tag{10}$$

$$F_{t1ij} = F_{t2ij} \tag{11}$$

In brittle material cutting, the depth of cut will be larger than the critical cutting depth when the force exceeds a critical value. At this condition, plastic deformation and crack system will emerge, as shown in Fig. 9. The lateral crack contributes to removing material, while the median crack produces the subsurface damage. The interaction of the diamond abrasive and workpiece is complex. Generally, when the depth of cut is h_{ij} for the abrasive (indentation depth), the normal force required can be obtained by the following equation [28]:

$$F_{n1ij} = \frac{1}{2}\pi H_1 h_{ij}^2 \left(\tan\theta_{ij}\right)^2 \tag{12}$$

where H_1 is hardness of workpiece, θ_{ij} is the half tip angle of the abrasive, and h_{ij} is depth of cut.

The abrasive particle will be pressed into the resin layer at a certain distance when it is forced. This displacement is small because the force is very little. The deformation of the resin layer is so little that we can assume that the interaction of the abrasive and the resin layer is elastic deformation. When the distance of the abrasive pressed into the resin layer is known, the normal force F_{n2ij} can be expressed as [29]

$$F_{n2ij} = \frac{\sqrt{8d_{ij}}}{3} E_2 \Delta h_{ij} \tag{13}$$

where d_{ij} is the diameter of the abrasive particle and E_2 is the elastic modulus of the resin layer. From Eq. (13), it can be seen that the displacement Δh_{ij} depends on the diameter of the abrasive particle, the elastic modulus of the resin layer, and the normal force.

The forces acting on the abrasive by workpiece and resin layer are obtained through Eqs. (12) and (13). Substituting the

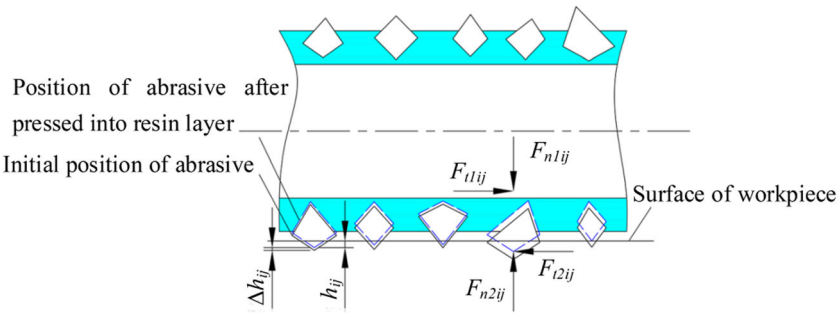

Fig. 8 Forces and displacement during cutting

two equations into Eq. (10), the relationship between depth of cut h_{ij} and displacement of the abrasive pressed into the resin layer Δh_{ij} is obtained:

$$\Delta h_{ij} = \frac{3\pi H_1 \left(h_{ij}\tan\theta_{ij}\right)^2}{2\sqrt{8d_{ij}}E_2} \tag{14}$$

2.4 Depth of cut for a single abrasive

In the process of resin bonded diamond wire sawing, the wire will bow at a certain degree due to its elastic property. Generally, the bow angle is less than 5°. Because the length of the workpiece is not long compared with wire length, the wire contacting with the workpiece can be seen as straight. Some assumptions are made in this paper: (1) the bottom of groove is a half circle and (2) there is no offset for wire on both sides. Taking arbitrary wire cross section, as shown in Fig. 10, the abrasive particles randomly distribute on the half bottom of the wire.

We assume that all the wire cross sections move downward with the displacement s. In Fig. 10, on the jth wire cross section, the depth of cut for the abrasive particle with the largest protrusion height is h_{maxj} and the displacement of the abrasive pressed into the resin layer is Δh_{maxj}. We can obtain the relationship between s, Δh_{maxj}, and h_{maxj}:

$$s\sin\alpha_{\max j} = h_{\max j} + \Delta h_{\max j} \tag{15}$$

From Eq. (14), we obtain

$$\Delta h_{\max j} = \frac{3\pi H_1 \left(h_{\max j}\tan\theta_{\max ij}\right)^2}{2\sqrt{8d_{\max j}}E_2} \tag{16}$$

Setting $\frac{3\pi H_1 \left(\tan\theta_{ij}\right)^2}{2\sqrt{8d_{ij}}E_2} = B_{ij}$, Eq. (16) can be expressed as

$$\Delta h_{\max ij} = B_{\max j} h_{\max j}^2 \tag{17}$$

Substituting Eq. (17) into Eq. (15), and solving this equation, we can get

$$h_{\max j} = \frac{-1 + \sqrt{1 + 4B_{\max j} s\sin\alpha_{\max j}}}{2B_{\max j}} \tag{18}$$

The depth of cut for an arbitrary particle on jth wire cross section is

$$h_{ij} = s\sin\alpha_{ij} - \left(H_{\max j} - H_{ij}\right) - \Delta h_{ij} \tag{19}$$

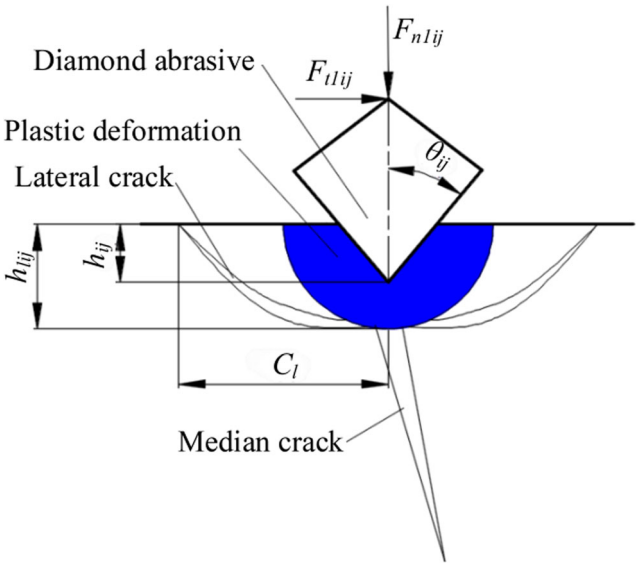

Fig. 9 Crack system for indentation fracturing

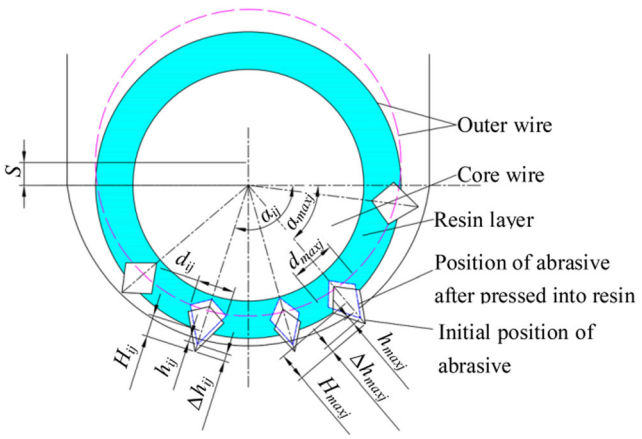

Fig. 10 The cutting depth of arbitrary particle on the jth wire cross section

Substituting Eq. (14) into Eq. (19), we get

$$h_{ij} = s\sin\alpha_{ij} - \left(H_{\max j} - H_{ij}\right) - B_{ij}h \tag{20}$$

By solving Eq. (20), the depth of cut for an arbitrary abrasive is

$$h_{ij} = \frac{-1 + \sqrt{1 + 4B_{ij}\left(s\sin\alpha_{ij} - H_{\max j} + H_{ij}\right)}}{2B_{ij}} \tag{21}$$

From Formula (21), it can be seen that h_{ij} depends on the maximum protrusion height of the abrasive on each cross section, its protrusion height on the jth wire cross section, the position angle, the elastic modulus of the resin layer, and the material property of the workpiece.

Based on the study of Lee [30], there are four distinct regimes occurring with the increase of depth of cut before brittle cutting: no wear, adhering, ploughing, and cutting. In the no wear and adhering regime, the workpiece only generates elastic deformation, while in the ploughing regime, it starts to show plastic deformation. All the three regimes do not remove material. Further increasing the depth of cut, chips begin to appear. This is ductile regime cutting, and the crack will occur for brittle cutting if the depth of cut increases. Because the depth of cut for the three cutting regimes is very small, we only consider the ductile cutting and brittle cutting modes.

The critical depth for transition from ductile to brittle mode of cutting depends on many factors, such as crystallographic orientation, abrasive shape, abrasive size, tip radius of abrasive, and cutting conditions. From many experimental results, it can be found that the critical depth for single crystal silicon is different due to the different cutting conditions. Prior work has established an empirical formula to calculate the critical depth based on the study of Bifano et al. [31]:

$$d_c = 0.15\left(\frac{E}{H}\right)\left(\frac{K_C}{H}\right)^2 \tag{22}$$

This expression is useful, although it does not explicitly account for the effects of scriber tip geometry, friction, etc. In this paper, the tip angle is random, so the critical depth of brittle-to-plastic transition for single crystal silicon should be different. However, it is very difficult to quantitatively describe the relationship between critical depth and tip angles and tip radius. The effects of these factors are just in qualitative researches by many experiments. To simplify the model, the critical depth of brittle-to-plastic transition for single crystal silicon is considered as a constant value. The corresponding corrections of this part are shown in the paper. The critical cutting depth of single crystal silicon is taken 0.5 μm according to the research of Chao [32].

According to Eq. (21), we can get the depth of cut for each abrasive particle. If $0 < h_{ij} \le 0.5$ μm, the cutting regime is in ductile mode. Moreover, the cross section area of the material which is removed by the abrasive is

$$S_{ij} = \frac{1}{2}h_{ij}^2\tan\theta_{ij} \tag{23}$$

The cutting regime is in brittle mode when $h_{ij} \ge 0.5$ μm. Moreover, the material is removed by lateral crack propagation. The length of lateral crack is obtained by the following Eq. [33]:

$$c_{lij} = \frac{\left(\cot\theta_{ij}\right)^{5/12}}{\left(\frac{\pi}{2} - \mu\cot\theta_{ij}\right)^{5/8}} \frac{{E_1}^{5/12}}{K_{IC}^{1/2}\sigma_y^{13/24}} F_{n1ij}^{5/8} \tag{24}$$

The depth of lateral crack is equal to the depth of plastic zone [34]:

$$h_{lij} = \left(\frac{\xi_L^{1/2}}{M^{1/4}}\right)\left(\cot\theta_{ij}\right)^{5/12} \frac{{E_1}^{5/12}}{K_{IC}^{1/2}{H_1}^{1/2}} F_{n1ij}^{5/8} \tag{25}$$

where E_1 is Young's modulus of single crystal silicon, K_{IC} is fracture toughness, σ_y is yield stress, H_1 is the hardness of single crystal silicon, and F_{n1ij} can be obtained by Formula (12). ζ_L is equal to 25×10^{-3}, and M is 3/4.

The cross section area which is removed by brittle fracturing is

$$S_{ij} = c_{lij}h_{cij} \tag{26}$$

The total cross section area removed by all abrasive particles in wire sawing is

$$S_{sum} = \sum S_{ij} \tag{27}$$

In unit time, the volume of material removed by all abrasive particles in processing is

$$V_1 = v_s\sum S_{ij} \tag{28}$$

Moreover, the volume of wire move downward is

$$V_2 = \frac{\pi Dl}{2}v_f \tag{29}$$

In theory, the two volumes should be equal:

$$v_s\sum S_{ij} = \frac{\pi Dl}{2}v_f \tag{30}$$

By Eqs. (18), (23), (24), (25), (26), and (27), it is observed that there is only one unknown parameter s in Eq. (29). Here, the iterative method is used to solve this equation. Thus, the depth of cut for each abrasive can be obtained. The normal force on each abrasive can be obtained by Eq. (12). Based on

the study of Chung et al. [7], the tangential force, when the depth of cut for abrasive is h_{ij}, is

$$F_{t1ij} = \begin{cases} H_1 h_{ij}^2 \tan\theta_{ij} & (0 < h_{ij} < 0.5) \\ 2H_1 C_l h_l & (h_{ij} \geq 0.5) \end{cases} \quad (31)$$

The total normal force and total tangential force are

$$\begin{cases} F_N = \sum F_{n1ij} \\ F_T = \sum F_{t1ij} \end{cases} \quad (32)$$

3 Simulation procedure

The simulation procedure of the established model is shown in Fig. 11. The input parameters are shown in Table 2. At first, the random positions of abrasive particles are generated, and then the abrasive particle with maximum protrusion height in each cross section is found and its position is recorded at the same time. Next, an initial value of s is given and the two volumes of material removed by total abrasives and wire are calculated, stopping the calculation if the two values meet the error demand; if not, the calculation is continued until this demand is satisfied. At last, the depths of cut for all abrasives are recorded, and the total normal force and total tangential force are calculated.

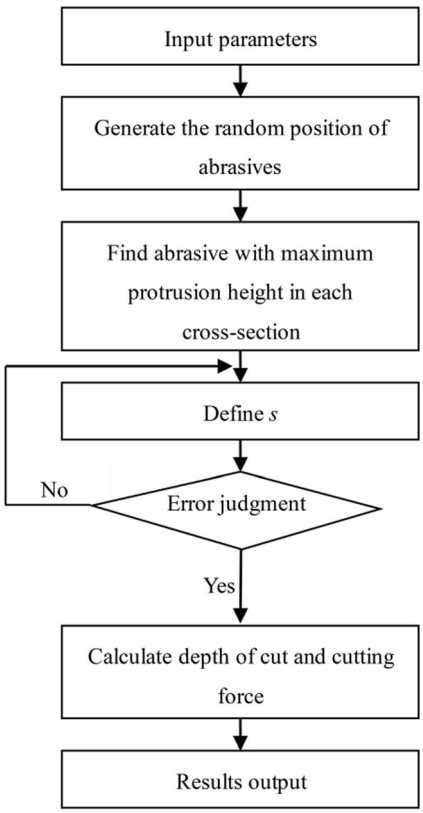

Fig. 11 Simulation procedure of proposed model

Table 2 Input parameters in simulation

Parameters	Value
Wire outer diameter (D/μm)	250
Length of workpiece (l/m)	0.1
Mean diameter of abrasives (d_m/μm)	50
Standard deviation (σ)	3.33
Hardness of silicon (H_1/GPa)	10
Elastic modulus of silicon (E_1/GPa)	127
Elastic modulus of resin (E_2/GPa)	1
Yield stress of silicon (σ_y/GPa)	3.8
Fracture toughness of silicon (K_{IC}/MPa)	0.7

4 Results and discussion

4.1 Model verification

The simulation was operated by MATLAB program. In order to verify the proposed calculation model, the same computational conditions were used in [18]. The elasticity of the resin layer was not considered; that is to say, the distance of the abrasive pressed into the resin layer is zero ($\Delta h = 0$). Besides that, all abrasive grits were cone, and the tip angle was 90°. Three simulations were done. The results obtained by reference and the proposed model are listed in Table 3.

From Table 3, it can be seen that the calculation results approach to the data from the reference. The maximum error is in simulation no.2, which is 6.89 %. The maximum error is small, so the correctness of the proposed model is proved.

4.2 Depth of cut for abrasive

Different parameter combinations were used to calculate the average depth of cut. Four feed rates (2, 4, 6, and 8 μm) and four wire speeds (2, 3, 4, and 5 m/s) were used in program calculation. Each simulation was calculated five times, and the average value was taken as the final result.

Table 3 Comparison of simulation results between reference and this paper

Simulation no.	v_s (m/s)	v_f (μm/s)	Average cutting depth (μm)		
			Reference	Proposed model	Relative error
1	5	6.25	0.68	0.71	4.41 %
2	10	6.25	0.58	0.54	6.89 %
3	10	12.5	0.70	0.72	2.86 %

The abrasives which contribute to removing material are defined as active abrasives. The average depth of cut for active abrasives with different feed rates and wire speeds are shown in Figs. 12 and 13. In the two figures, $\Delta h = 0$ means that the elasticity of the resin layer is not considered, that is to say, the wire can be seen as electroplated diamond wire. On the contrary, the elasticity of the resin layer is considered at the condition of $\Delta h \neq 0$. From these two figures, the average depth of cut under the condition of $\Delta h \neq 0$ is less than that at the condition of $\Delta h = 0$, despite the changes of wire speed and feed rate. In other words, the average depth of cut for resin bonded wire saw is less than that in electroplated diamond wire saw at the same processing parameters. This result is similar to the experimental results obtained by Tsai et al. [3].

During the resin bonded diamond wire sawing, the active abrasives are forced by the workpiece and the resin layer of the wire. As discussed previously, the active abrasive particles are penetrated into the workpiece and pressed into the resin layer at the same time. This leads to their protrusion heights which tend to be uniform. So, more abrasive particles take part in removing material, which result in smaller average depth of cut and generating a better surface quality, shorter lateral crack, and less machining damage. This is very beneficial to the as-cut silicon wafers when the thickness of wafer decreases.

The effects of feed rate and wire speed on the average depth of cut also can be seen in Figs. 12 and 13. The average depth of cut increases with the increase of feed rate, while it decreases with the increase of wire speed. This can be explained by Figs. 14 and 15. The cutting regime for the abrasive is changed with the different feed rates and wire speeds. With the increase of feed speed, the number of abrasives in brittle cutting regime increases. This indicates that the mechanism of material removal changes from ductile mode to brittle mode for some abrasive particles. The opposite phenomenon occurs

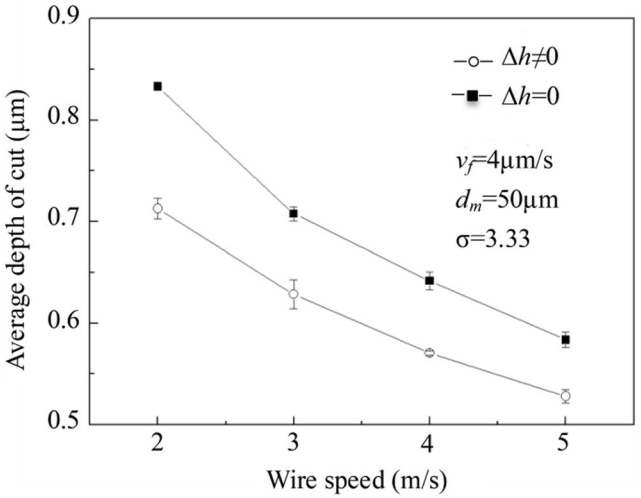

Fig. 13 Average depth of cut with different wire speeds at two conditions

when the wire speed increases. In both cases, most of abrasives are in brittle cutting. So, the brittle cutting regime is the major way of material removal.

The average depths of cut for abrasive particles on different wire cross section positions are different as shown in Fig. 16. In this figure, the average depth of cut for all the active particles at the same position angle in different cross sections is statistically calculated. From Fig. 16, it can be seen that the average depth of cut increases first and then decreases with the increase of the position angle. The abrasive particles at the bottom have the largest average depth of cut. Based on the study of Gao [16] and Chung [18], the material removal hugely depends on the abrasives at the bottom, forming the kerf. In contrast, the wafer surface is generated by the abrasives at the side contributing to little material removal. The average depth of cut for abrasive particles at the side is less. If diamond wire sawing is under the condition of optimum processing parameter combination, the depth of cut for abrasive at the side may realize the ductile cutting and get a better cutting surface.

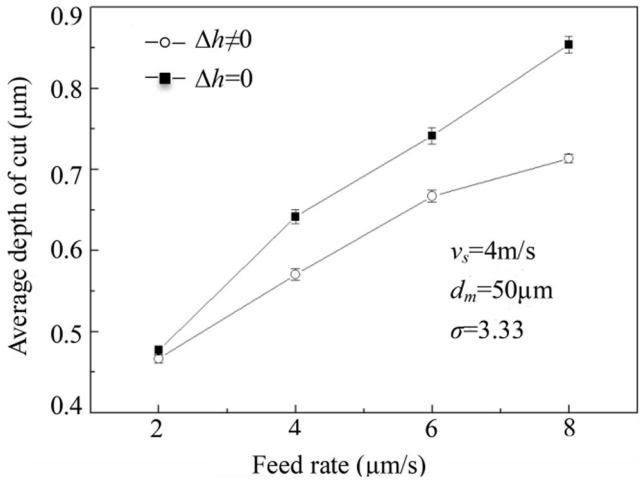

Fig. 12 Average depth of cut with different feed rates at two conditions

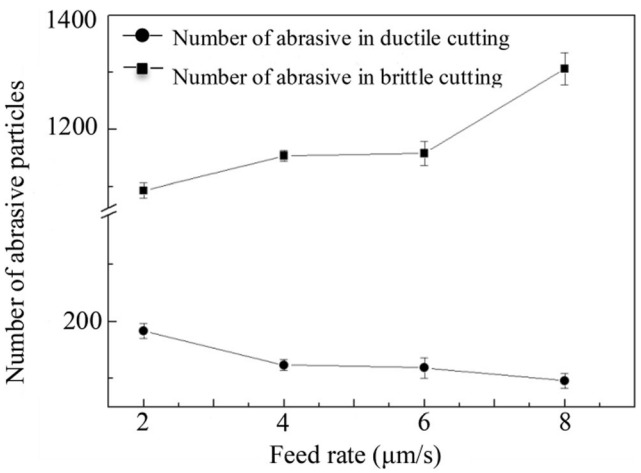

Fig. 14 Change of number of active abrasives with feed speed

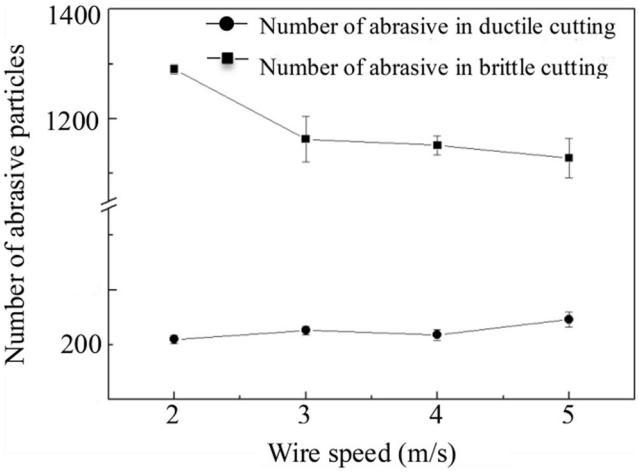

Fig. 15 Change of number of active abrasives with wire speed

4.3 Cutting force

The cutting force for resin bonded diamond wire saw is an important index which can affect the micromachining features of abrasive particles, the abrasion of resin layer, etc. Establishing the relationship between cutting forces and processing parameters is the basis of analyzing processing characteristic and cutting quality. So far, an accurate and feasible formula is absent for resin bonded diamond wire saw. One method for establishing the mathematical relationship is doing lots of cutting experiments to measure the cutting force. The general formula can be expressed as the following equations [35]:

$$\begin{cases} F_N = C_1 (v_f)^{\alpha_1} (v_s)^{\alpha_2} (D)^{\alpha_3} (l)^{\alpha_4} \\ F_T = C_2 (v_f)^{\beta_1} (v_s)^{\beta_2} (D)^{\beta_3} (l)^{\beta_4} \end{cases} \tag{33}$$

where C_1, C_2, α_1, α_2, α_3, α_4, β_1, β_2, β_3, and β_4 are undetermined coefficients.

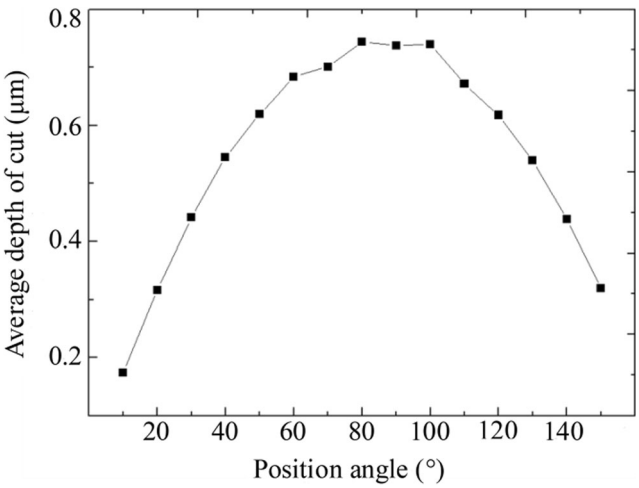

Fig. 16 Average depth of cut for abrasives with different position angles

During wire sawing, many factors have effects on cutting force. The main factors are feed rate, wire speed, the length of workpiece, diameter of wire, etc. In order to obtain a mathematical relationship between processing parameters and cutting force, 50 simulations of different parameter combinations have been done. The least squares method is used to obtain the model coefficients, and the proposed model is

$$F_N = 0.141 \times \frac{v_f^{0.728}}{v_s^{0.656}} D^{1.017} l^{0.975} \tag{34}$$

The correlation coefficient of this model is 0.9793. From Formula (34), it can be seen that there is a positive correlation between cutting forces and feed rate, wire diameter, and length of workpiece, while cutting forces and wire speed have a negative correlation. The total normal force and the total tangential force increase with the increasing of feed rate, diameter of wire, and the length of workpiece. However, these two forces decrease with the increase of wire speed. The force ratio F_N/F_T is about 1.2; this value is in the range of 0.3~1.3 obtained by Hardin [22].

As discussed previously, the depth of cut for abrasive particles, which is determined by the cutting force, will increase if the feed rate becomes larger. Therefore, the cutting force increases with the increase of the feed rate. Increasing the wire diameter and the length of wire contact with the workpiece will increase the total abrasive number. More abrasive particles take part in cutting materials resulting in the increase of the cutting force. The depth of cut decreases with the increase of wire speed. This leads to the decrease of the cutting force.

5 Conclusion

A model of studying depth of cut for abrasive particles and cutting force for resin bonded diamond wire saw is developed. The elasticity of the resin layer and the random distribution character of abrasive particles are considered in this proposed model. The model can calculate depth of cut and cutting force for two kinds of diamond wire saw: electroplated diamond wire saw and resin bonded diamond wire saw. The conclusions are as follows:

1. The average depth of cut for abrasive particles in resin bonded diamond wire sawing is less than that in electroplated diamond wire sawing at the same-parameter combination.
2. The depths of cut for abrasive particles with different position angles are different. The brittle cutting is the major way of material removal.
3. A mathematical relationship between processing parameters and cutting force is obtained. The force ratio of total normal force to tangential force is about 1.2. Feed rate,

wire diameter, and length of workpiece have a positive correlation on cutting force, while wire speed has a negative correlation on cutting force.

Acknowledgment This work is supported by the Shandong Provincial Natural Science Foundation of China (ZR2014EEM034) and the National Natural Science Foundation of China (Nos. 51075240 and 51205234).

Reference

1. Kao I (2004) Technology and research of slurry wiresaw manufacturing systems in wafer slicing with free abrasive machining. Int J Adv Manuf Syst 7(2):7–20
2. Chung C, Tsay GD, Tsai MH (2014) Distribution of diamond grains in fixed abrasive wire sawing process. Int J Adv Manuf Technol 73(9-12):1485–1494
3. Tsai PH, Chou YC, Yang SW, Chen YC, Wu CH (2013) A comparison of wafers sawn by resin bonded and electroplated diamond wire—from wafer to cell. Photovoltaic Specialists Conference (PVSC). doi:10.1109/PVSC.2013.6744204
4. Watanabe N, Kondo Y, Ide D, Matsuki T, Takato H, Sakata I (2010) Characterization of polycrystalline silicon wafers for solar cells sliced with novel fixed-abrasive wire. Prog Photovoltaics 18(7):485–490
5. Wu H, Melkote SN (2012) Study of ductile-to-brittle transition in single grit diamond scribing of silicon: application to wire sawing of silicon wafers. J Eng Mater Technol 134(4):041011
6. Gao YF, Ge PQ, Li SJ (2009) Investigation of subsurface damage depth of single crystal silicon in electroplated wire saw slicing. Key Eng Mater 416:306–310
7. Möller HJ (2004) Basic mechanisms and models of multi-wire sawing. Adv Eng Mater 6(7):501–513
8. Teomete E (2011) Effect of process parameters on surface quality for wire saw cutting of alumina ceramic. GU J Sci 24(2):291–297
9. Li Z, Wang MJ, Pan X, Ni YM (2015) Slicing parameters optimizing and experiments based on constant wire wear loss model in multi-wire saw. Int J Adv Manuf Technol 81(1-4):329–334
10. Lee S, Kim H, Kim D, Park C (2015) Investigation on diamond wire break-in and its effects on cutting performance in multi-wire sawing. Int J Adv Manuf Technol. doi:10.1007/s00170-015-7984-3
11. Qiu T, Yao C, Zhang W, Tang C, Peng W, Wang Y (2016) Experimental study of the cutting performance of free-abrasive wire sawing in a magnetic field. Int J Adv Manuf Technol. doi:10.1007/s00170-016-8719-9
12. Li J, Kao I, Prasad V (1998) Modeling stresses of contacts in wire saw slicing of polycrystalline and crystalline ingots: application to silicon wafer production. J Electron Packag 120(2):123–128
13. Liedke T, Kuna M (2011) A macroscopic mechanical model of the wire sawing process. Int J Mach Tool Manuf 51(9):711–720
14. Liedke T, Kuna M (2013) Discrete element simulation of micromechanical removal processes during wire sawing. Wear 304(1–2):77–82
15. Nassauer B, Hess A, Kuna M (2014) Numerical and experimental investigations of micromechanical processes during wire sawing. Int J Solids Struct 51(14):2656–2665
16. Gao YF, Ge PQ (2012) Relationship between the grit cut depth and process parameters in electroplated diamond wire sawing KDP crystal. Appl Mech Mater 101:950–953. doi:10.4028/www.scientific.net/AMM.101-102.950
17. Chung C, Le VN (2014) Generation of diamond wire sliced wafer surface based on the distribution of diamond grits. Int J Precis Eng Manuf 15(5):789–796
18. Chung C, Le VN (2015) Depth of cut per abrasive in fixed diamond wire sawing. Int J Adv Manuf Technol 80(5):1137–1346
19. Yang F, Kao I (2001) Free abrasive machining in slicing brittle materials with wiresaw. J Electron Packaging 123(3):254–259
20. Clark WI, Shih AJ, Hardin CW, Lemaster RL, McSpadden SB (2003) Fixed abrasive diamond wire machining—part I: process monitoring and wire tension force. Int J Mach Tool Manuf 43(5):523–532
21. Clark WI, Shih AJ, Lemaster RL, McSpadden SB (2003) Fixed abrasive diamond wire machining—part II: experiment design and results. Int J Mach Tool Manuf 43(5):533–542
22. Hardin CW, Qu J, Shih AJ (2004) Fixed abrasive diamond wire saw slicing of single-crystal silicon carbide wafers. Mater Manuf Process 19(2):355–367
23. Li SJ, Zhang J, Wan B, Li Y (2012) The force theoretical analysis and experiment for wire saw with UVM cutting SiC monocrystal. Appl Mech Mater 117:1728–1735. doi:10.4028/www.scientific.net/AMM.117-119.1728
24. Gao YF, Ge PQ, Hou ZJ (2008) Study on removal mechanism of fixed-abrasive diamond wire saw slicing monocrystalline silicon. Key Eng Mater 359:450–454. doi:10.4028/www.scientific.net/KEM.359-360.450
25. Xie Y, Bhushan B (1996) Effects of particle size, polishing pad and contact pressure in free abrasive polishing. Wear 200(1):281–295
26. Sung CM (1999) Brazed diamond grid: a revolutionary design for diamond saws. Diam Relat Mater 8(8):1540–1543
27. Bidiville A, Wasmer K, Michler J, Nasch PM et al (2010) Mechanisms of wafer sawing and impact on wafer properties. Prog Photovoltaics 18(8):563–572
28. Williams J (2005) Engineering tribology. Cambridge University, New York
29. Lv X (2010) Theoretical study on high efficiency and ductile regime lapping of semi-fixed abrasive plate doctoral dissertation. Zhejiang University of Technology, China, Dissertation
30. Lee SH (2012) Analysis of ductile mode and brittle transition of AFM nanomachining of silicon. Int J Mach Tool Manuf 61:71–79
31. Bifano TG, Dow TA, Scattergood RO (1991) Ductile-regime grinding: a new technology for machining brittle materials. J Eng Ind 113(2):184–189
32. Chao CL, Ma KJ, Liu DS (2002) Ductile behaviour in single-point diamond-turning of single-crystal silicon. J Mater Process Technol 127(2):187–190
33. Marshall DB, Lawn BR, Evans AG (1982) Elastic/plastic indentation damage in ceramics: the lateral crack system. J Am Ceram Soc 65(11):561–566
34. Evans AG, Gulden ME, Rosenblatt M (1978) Impact damage in brittle materials in the elastic-plastic response regime. Proceed Royal Soc London A 361(1706):343–365. doi:10.1098/rspa.1978.0106
35. Liu Q, Chen X, Wang Y, Gindy N (2008) Empirical modelling of grinding force based on multivariate analysis. J Mater Process Technol 203(1):420–430